

AD-A136 798

ROLE OF AL₂O₃ IN SINTERING OF SUBMICRON
YTTRIA-STABILIZED ZRO₂ POWDERS(U) ILLINOIS UNIV AT
URBANA DEPT OF CERAMIC ENGINEERING R C BUCHANAN ET AL.
02 DEC 83 N00014-80-K-0969 F/G 11/6

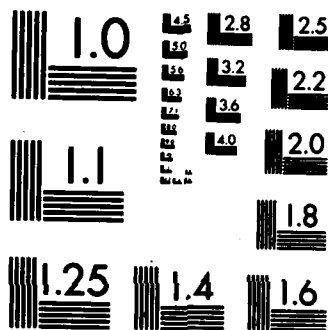
1/1

UNCLASSIFIED

F/G 11/6

NL

ENC



MICROCOPY RESOLUTION TEST CHART
NATIONAL BUREAU OF STANDARDS-1963-A

12

Final Report
Technical Report No. 8
Contract No.: US NAVY-N-00014-80-K-0969

ROLE OF Al_2O_3 IN SINTERING OF SUBMICRON
YTTRIA-STABILIZED ZrO_2 POWDERS

A136798

DTIC FILE COPY



DTIC

JAN 13 1984

A

DEPARTMENT OF CERAMIC ENGINEERING
UNIVERSITY OF ILLINOIS
URBANA, ILLINOIS

This document has been approved
for public release and sale; its
distribution is unlimited.

83 12 21 012

Final Report
Technical Report No. 8
Contract No.: US NAVY-N-00014-80-K-0969

ROLE OF Al_2O_3 IN SINTERING OF SUBMICRON
YTTRIA-STABILIZED ZrO_2 POWDERS

by

R. C. Buchanan and D. M. Wilson

December 1983

Department of Ceramic Engineering
University of Illinois at Urbana-Champaign
Urbana, IL 61801

DTIC
JAN 13 1984
A

This research was supported by the Office of Naval Research
Department of the Navy
Contract No. US NAVY-N-00014-80-K-0969

Reproduction in whole or in part is permitted for any purpose
of the United States Government

This document has been approved
for public release and sale; its
distribution is unlimited.

REPORT DOCUMENTATION PAGE		READ INSTRUCTIONS BEFORE COMPLETING FORM
1. REPORT NUMBER 8	2. GOVT ACCESSION NO. A136798	3. RECIPIENT'S CATALOG NUMBER
4. TITLE (and Subtitle) Role of Al_2O_3 in Sintering of Submicron Yttria-Stabilized ZrO_2 Powders		5. TYPE OF REPORT & PERIOD COVERED Interim Research Report Oct. 1980-Sept. 30, 83 Nov. 30, 1983
7. AUTHOR(s) R. C. Buchanan and D. M. Wilson		6. PERFORMING ORG. REPORT NUMBER
9. PERFORMING ORGANIZATION NAME AND ADDRESS University of Illinois at Urbana-Champaign Department of Ceramic Engineering 105 S. Goodwin, Urbana, IL 61801		8. CONTRACT OR GRANT NUMBER(s) US NAVY-N-00014-80-K-0969
11. CONTROLLING OFFICE NAME AND ADDRESS Office of Naval Research, Metallurgy 800 N. Quincy Ave., Arlington, VA 22217		10. PROGRAM ELEMENT, PROJECT, TASK AREA & WORK UNIT NUMBERS ONR-Metallurgy Code 471
14. MONITORING AGENCY NAME & ADDRESS (if different from Controlling Office) same as control office		12. REPORT DATE December 2, 1983
		13. NUMBER OF PAGES
		15. SECURITY CLASS. (of this report) Unclassified
		15a. DECLASSIFICATION/DOWNGRADING SCHEDULE
16. DISTRIBUTION STATEMENT (of this Report) widespread; required numbers of copies to defense documentation center; individuals and organization on approved distribution list furnished by Metallurgy and Ceramic Program--ONR		
17. DISTRIBUTION STATEMENT (of the abstract entered in Block 20, if different from Report) same		
18. SUPPLEMENTARY NOTES none		
19. KEY WORDS (Continue on reverse side if necessary and identify by block number) YSZ, zirconia, densification, translucency, liquid phase sintering		
20. ABSTRACT (Continue on reverse side if necessary and identify by block number) see other side		

ABSTRACT

The use of Al_2O_3 (up to ~2vol%) as a sintering aid to promote rapid densification of precipitated yttria (8.0 wt.%) stabilized Zirconia (YSZ) powders in the range 1100°-1350°C, was investigated. The Al_2O_3 was added as hydrated $\text{Al}(\text{OH})_3$ and dispersed by milling in a 60 : 40 alcohol : water solution, followed by pressing at 205 MPa. Significantly increased densification was obtained with Al_2O_3 , even below 1200°C, and optimum densification (>99.0% Th.D.) occurred at 1350°C/1 hr. with 0.325 wt.% Al_2O_3 . Sintered samples exhibited enhanced electrical conductivity and larger grain size (0.3 - 0.5 μm). TEM microstructural observations and densification kinetic data indicated a liquid phase assisted sintering mechanism. Solid state doping of the ZrO_2 by Al was inferred from the electrical conductivity data.

Role of Al_2O_3 in Sintering of Submicron
Yttria-Stabilized ZrO_2 Powders

by

R. C. Buchanan and D. M. Wilson
Department of Ceramic Engineering
University of Illinois at Urbana-Champaign
Illinois, 61801

ABSTRACT

→ The use of Al_2O_3 (up to ~3.5 wt%) as a sintering aid to promote rapid densification of precipitated yttria (8.0 wt. %) stabilized Zirconia (YSZ) powders in the range $1100^\circ\text{--}1350^\circ\text{C}$, was investigated. The Al_2O_3 was added as hydrated $\text{Al}(\text{OH})_3$ and dispersed by milling in a 60 : 40 alcohol : water solution, followed by pressing at 205 MPa. Significantly increased densification was obtained with Al_2O_3 , even below 1200°C , and optimum densification (>99.0% Th.D.) occurred at $1350^\circ\text{C}/1$ hr. with 0.325 wt% Al_2O_3 . These samples exhibited enhanced electrical conductivity and larger grain size (0.3 - 0.5 μm). TEM microstructural observations and densification kinetic data indicated a liquid phase assisted sintering mechanism. Solid state doping of the ZrO_2 by Al was inferred from the electrical conductivity data. ←

A



Accession For	
NTIS GR&I	<input checked="" type="checkbox"/>
DTIC TAB	<input type="checkbox"/>
Unannounced	<input type="checkbox"/>
Justification	<input type="checkbox"/>
Distribution/	
Availability Codes	
Avail and/or	
Spec. Avail	
A1	

INTRODUCTION

The beneficial effect of Al_2O_3 on the sintering of stabilized zirconia has been noted by several investigators^{1,2}. However, the mechanism for the observed densification increases has yet to be adequately explained. An additive such as Al_2O_3 can be accommodated in a host material in one of three distinct ways: as a solid solution dopant, as a grain boundary segregant or as a discrete second phase. Combinations of these mechanisms, as determined by the thermodynamics and kinetics of the system, are also possible.

With many additive systems, densification is affected by the formation of an intergranular liquid phase. This contributes to particle rearrangement through grain boundary sliding, assists in the dissolution of particle-particle contacts and in some cases provides a pathway for rapid mass transport during sintering. Significant enhancement in the densification behavior of ceramic systems have been observed with liquid contents ≤ 1.0 vol%^{3,4} and capillary forces are largest for small liquid contents.⁵ The effectiveness of the intergranular phase is strongly dependent on its composition as liquid phase kinetics can be determined by the solution of the solid particles in the melt phase. The presence of an intergranular phase in the fired body can, however, be detrimental to such properties as high temperature strength⁶ and electrical conductivity^{7,8}, both of critical importance for electrolyte applications.

Other additives may enhance sintering without the formation of an intergranular liquid phase. Dopants soluble in the host lattice can enhance densification by increasing the defect concentration of the diffusing

species. Thus, Harmer et al,⁹ attributed increased sintering of high purity Al_2O_3 (Al^{3+} lattice diffusion controlled) doped with Ti^{4+} to an increase in the aluminum vacancy concentration. Conversely, Mg^{2+} additions promoted sintering by the formation of Al^{3+} interstitials.

Densification enhancement for segregated dopants can be attributed to such effects as decreased grain boundary to surface energy ratios¹⁰ or to reduced grain boundary mobility due to the presence of discrete solid second phases, pores or segregated solutes. In those systems with a preference for grain boundary diffusion, sintering may also be affected by changes in the amount and nature of the boundary impurities. Segregated impurities have been shown to significantly reduce grain boundary electrical conductivity in YSZ^{11,12,8}, possibly due to trapping⁷ or to occupation of interstitial sites⁵⁰. Parallel effects may also exist for cationic diffusion.

In stabilized zirconias, the stabilizing oxide may be enriched on the grain boundary due to its affinity for a liquid phase¹⁴ or for a segregated additive. This is particularly likely in calcia-stabilized zirconia (CSZ) due to the high affinity of Ca for most grain boundary impurities. Thus, the distribution of an additive may be partially determined by existing impurities and solutes as well as by sintering temperature.

Alumina, although only 0.1 mol % soluble in YSZ at 1300°C¹³, can be dissolved up to 1-2 mol% at 1700°C¹². Bernard¹³ reported low grain boundary conductivities in samples cooled slowly to room temperature but conductivities equivalent to bulk values after rapid quenching.

Radford et al² (YSZ and CSZ), Mallinckrodt³ (CSZ) and Takagi¹⁶ (CSZ) all have attributed enhanced sintering with Al_2O_3 to a liquid phase formed by the dopant, the stabilizing oxide and existing impurities such as MgO , SiO_2 , and CaO . Assuming a sufficient impurity level, this is a plausible

interpretation, since numerous eutectics could be formed with the above-mentioned oxides below 1500°C and alumina has been found to be concentrated on the grain boundaries of CSZ along with associated Ca, Mg and Si impurities.^{8,16} Sintering temperatures investigated by the three investigators were in the range 1480°C to 1800°C.

Radford noted a densification enhancement in CSZ + Al₂O₃ both for nuclear grade (99.7% pure) and lower purity (~97%) technical grade samples. Mallinckrodt noted a density decrease in Al₂O₃ doped samples for the highest firing temperatures (1800°C). Although all zirconia sintering additives such as Al₂O₃, Fe₂O₃, TiO₂ and SiO₂ decreased conductivity,^{17,2} Radford reported that the decrease with Al₂O₃ additions was relatively small, especially for the lower purity samples. Takagi noted substantial grain growth with Al₂O₃ additions and Radford a decrease in grain size. This difference suggests that the effect of the Al₂O₃ on densification is dependent on sample purity and preparation as well as on firing conditions.

Liquid phase sintering was first refuted as a possible sintering mechanism by Bernard¹³. The beneficial effect of Al₂O₃ additions was found to be strong as low as 1100°C, well below temperatures where the liquid phase would normally be expected. Microstructural examination indicated that Al₂O₃ was present mainly as second phase inclusions and the grain boundaries were free of liquid. AC Impedance spectroscopy indicated a diminution of intergranular resistance with Al₂O₃ additions, and a net increase in conductivity was reported. This was attributed to increased grain size, which reduced the high resistivity grain boundary area. The Al₂O₃ additive level could be varied between 0.44 and 1.70 mol% without affecting electrical or densification behavior. Butler et al¹⁴ supported these conclusions and proposed that the Al₂O₃ particles acted as scavengers for intergranular

SiO_2 . As the grain boundaries moved past the (assumed stationary) Al_2O_3 inclusions, intergranular SiO_2 diffused rapidly to the Al_2O_3 particles due to the greater thermodynamic stability of mullite ($3\text{Al}_2\text{O}_3 \cdot 2\text{SiO}_2$) compared to zircon ($\text{ZrO}_2 \cdot \text{SiO}_2$), forming silica-rich cusps on the Al_2O_3 inclusions. Densification was attributed to grain boundary pinning by the Al_2O_3 inclusions. An increase in conductivity could be assumed due to the removal of amorphous second phases from the grain boundary. The presence of Al_2O_3 in YSZ as discrete inclusions was also reported by Rao et al.¹⁹ Silica was present at triple points and in < 20 nm thick films on grain boundaries, which were depleted in yttrium.

The presence of a continuous, segregated grain boundary phase was also reported by Verkerk et al. in a study of the electrical behavior of YSZ. Impurities such as Ca, Ti and sintering aids such as Fe_2O_3 and Al_2O_3 , which were considered to be enriched on the grain boundaries, reduced boundary conductivity significantly.²⁰

Early studies on the kinetics of sintering of $> 1 \mu\text{m}$ zirconia showed shrinkage time exponents to be near 0.50, which would indicate bulk diffusion control.^{21,22} Creep data has supported this conclusion²³. Nevertheless, Rhodes and Carter, while observing bulk diffusion control during sintering, found boundary diffusivities to be up to 10^5 times as high as bulk values²². Shrinkage exponents near 0.3 in a low temperature study using Cr_2O_3 -stabilized powders indicated the dominance of grain boundary diffusion²⁴. Young et al. also report grain boundary diffusion control in Zyttrite ($\sim 100\text{\AA}$ particle size YSZ)²⁵, while Wirth noted grain boundary control in submicron CSZ.²⁶ Changes in sintering pathway from lattice to grain boundary control as grain size decreases has been observed in both MgO and Al_2O_3 .²⁷ A grain boundary sintering mechanism in submicron YSZ would suggest considerable sensitivity to

segregated impurity ions and to amorphous or second phases.

In stabilized zirconias with large oxygen vacancy concentration, the cation diffusion would be rate controlling. Usually, cation vacancies are assumed, although zirconium interstitials have been identified, though only under high (1800°C) temperature conditions.²⁸ As pointed out by Brook,²⁹ compressive creep data³⁰ indicated a significant maximum creep rate in CSZ at 15 mol% CaO. This is very close to the point at which full stabilization is achieved, conductivity is at a maximum, and the free oxygen vacancy concentration is greatest. A diffusion rate maximum for zirconium under these conditions would be more consistent with zirconium interstitial control than with vacancy control.

Based on the above, the object of this investigation was to examine, mechanistically, the role of Al_2O_3 as a sintering aid for submicron stabilized ZrO_2 (YSZ) powders with a view to achieving lower densification temperatures and times, as well as improved optical and mechanical properties.

EXPERIMENTAL

The powder used in this study was commercially available submicron yttria (8.0 wt%; ~9.1 mol % $\text{Y}\text{O}_{1.5}$) stabilized zirconia (YSZ). Typical lot analysis and physical properties for the powders used are given in Table 1.

Residual chlorine, shown by Scott and Reed³¹ to inhibit densification, was removed by washing in distilled water. Dilute suspensions (1.0 vol %) were subjected to ultrasonic vibrations for 15 minutes, followed by centrifuging and decanting of the liquid. Chemical analysis, carried out by atomic absorption technique and by Hg titration for Cl, indicated a reduction in Cl content from 0.80 wt% to ≤ 0.04 wt%. Alumina, obtained from fine grained aluminum hydroxide ($\text{Al}(\text{OH})_3 \cdot 3\text{H}_2\text{O}$), 99.9% pure, was added as a sintering aid. The additive level of Al_2O_3 was varied from 0-3.24 wt% (3.92 mol%).

The as-received powders were ball milled for 12 hours with ZrO_2 balls in polyethylene jars to reduce agglomeration. Fig. 1 shows the considerable reduction in agglomerate size distribution from ~10-15 μm for the as-received to ~0.3-0.5 μm for the milled powder. Fig. 1B also shows, from the enhanced fine structure, crystallite sizes in the range 0.02-0.03 μm . The milled suspensions, with 1.0 wt% carbowax 4000 and 1.0 wt% PVA added as binders, were spray dried* and pellets of 1.6 cm diameter and ~0.15 cm thickness were pressed uniaxially at 220MPa. Figs. 1C and 1D show the spray dried and pressed morphologies. Firing was carried out on Pt foil on ZrO_2 setters in a MoSi_2 furnace in the range 1100°-1350°C from 1 min. to 24hr.

* Buchi Laboratory Spray Dryer, Brinkman Instruments, New Jersey

Table 1.

Typical Lot Analysis for Yttria Stabilized Zirconia (YSZ) Powders*

Composition (wt.%)

<u>Constituent</u>	<u>wt%</u>	<u>Constituent</u>	<u>wt%</u>
ZrO ₂	~90	NiO	0.03
Y ₂ O ₃	8.0	Fe ₂ O ₃	0.01
HfO ₂	1.6	SiO ₂	0.10
Al ₂ O ₃	0.04	TiO ₂	0.06
CaO	0.30	Na ₂ O	0.20
BaO	0.03	K ₂ O	0.02
MgO	0.01	Cl	~1.0

Physical Properties

Crystalline Phase	cubic
Crystalline Size	0.02-0.03 μm
Surface area (BET)	50 m ² /g

*Zircar Corp., Florida, New York, 10921

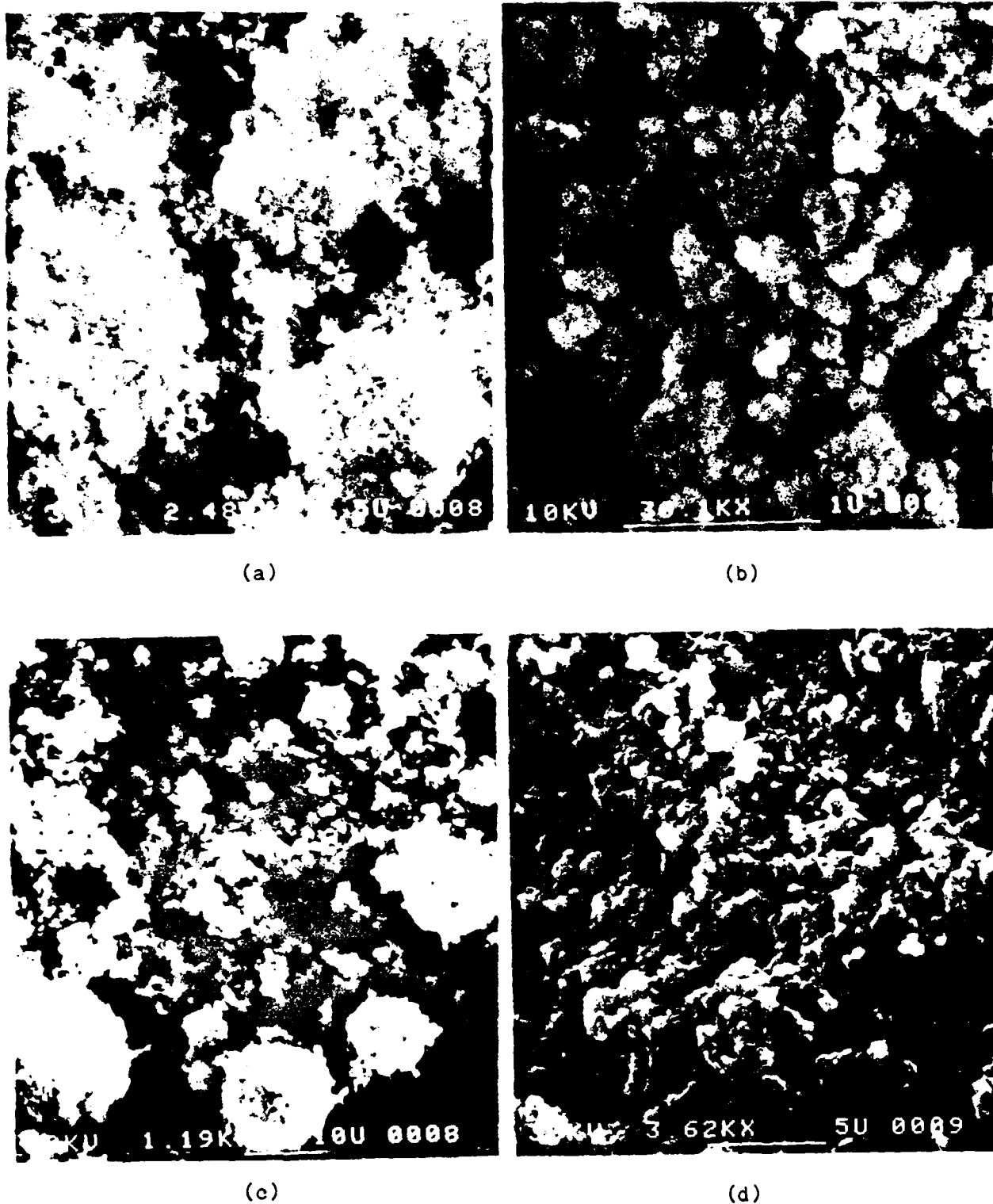


FIGURE 1. SEM Photomicrographs of YSZ Powders: a) As-Received b) Milled 14h c) Spray Dried d) Pressed at 230 MPa

Sintered densities were determined by the Archimedes technique. The theoretical density of YSZ (8.0 wt%) was calculated to be 6.022 g/cm^3 using the lattice parameter data of Tuohig.³² Calculated densities using a series mixing formula decreased progressively with added Al_2O_3 , the value for 0.65 wt% alumina being 6.00 g/cm^3 .

Microstructures were analyzed by SEM, TEM and EDAX microanalysis techniques. Grain sizes were determined from SEM photomicrographs of polished and thermally etched sections, using the line intersection technique of Mendelsohn.³³ TEM samples were prepared using a ball cratering device** followed by < 10 hr ion milling, thereby assuring a minimal of milling artifacts. DC electrical resistivity was measured using a Hewlett-Packard 4260A Universal bridge. Specimens were polished plane parallel and provided with Pt paste electrodes, which were fired at 800°C in air. Measurements were made, in air ambient, up to 900°C .

** VSZ Ball Cratering Instrument, The Technology Shop, Inc., Sudbury, Mass.

RESULTS AND DISCUSSION

Figure 2 shows the effect of Al_2O_3 additions (0-3.25 wt%) on the fired densities of precipitated YSZ powders at 1200°C and 1300°C for 1 hr. Densification at 1200°C was significantly enhanced by Al_2O_3 additions ≤ 0.65 wt%, with a similar effect noted at 1300°C where higher overall densities were achieved. Above 0.65 wt% Al_2O_3 additive content, a relative decrease in densification, more pronounced at 1300°C, was observed. This suggested the optimum Al_2O_3 additive content to YSZ to be in the range 0.3-0.65 wt%.

Fig. 3 compares, for even shorter soak times (0.5 hr), the relative densities achieved for YSZ and YSZ + 0.325 wt% Al_2O_3 samples at sintering temperatures between 1100° and 1350°C. The difference in density between the two samples is seen to increase as the sintering temperature was increased. However, both samples achieved > 90% theoretical density at 1350°C/0.5 hr. Fig. 4, compares the shrinkage behavior ($\log \Delta L/L_0$) as a function of time for the two samples in Fig. 3. The shrinkage data shown corresponded to relative density values in the range 65-92%. Shrinkage for the Al_2O_3 doped sample was higher than for the YSZ sample, in line with the higher densification rate, but the parallel shrinkage curves indicated a similar densification mechanism.

The nonlinearity of the sintering curves in Fig. 3 would indicate liquid phase densification with different amounts of liquid present. Likewise, the two slopes for the shrinkage curves coupled with the rapid densification rate would classically be interpreted as evidence for liquid phase sintering. Particle rearrangement would be predominant in the initial stages followed by a solution precipitation mechanism at longer sintering times. This behavior is evident from Fig. 5 which shows the changes in density with sintering time for the YSZ and Al_2O_3 doped samples sintered at 1200°C and 1275°C. For short soak

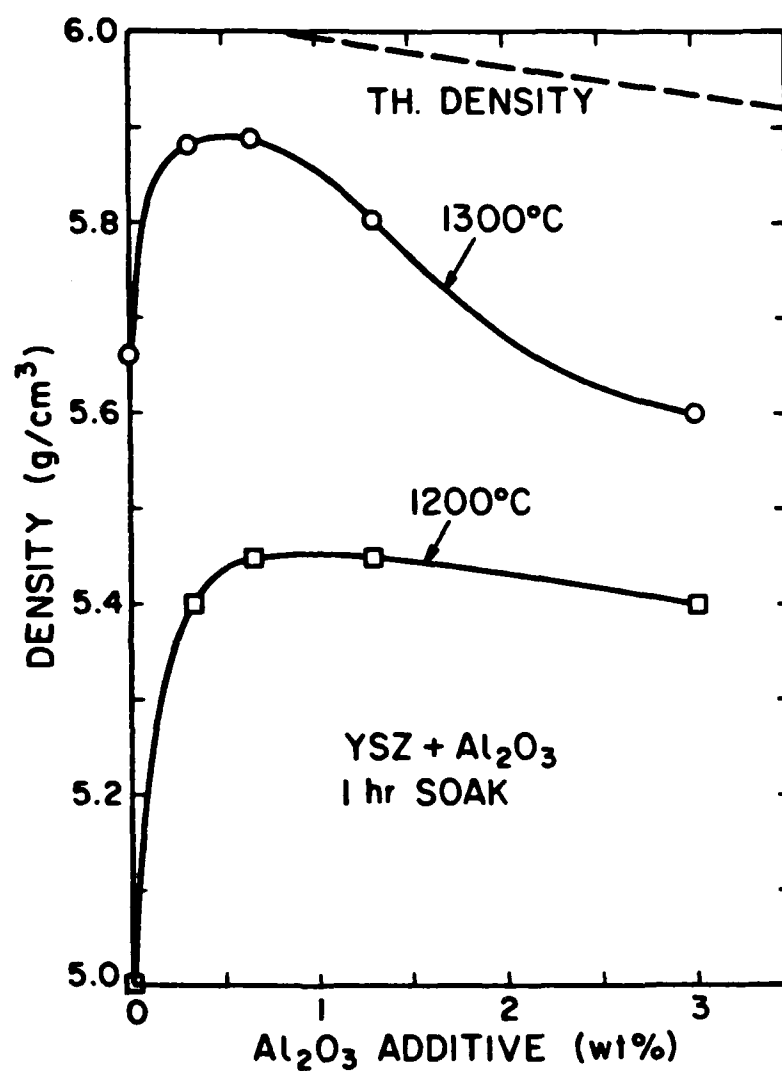


FIGURE 2. Plot of fired density for YSZ powder at 1200°C and 1300°C/1 hr., showing sintering enhancement with Al₂O₃ additions (wt%).

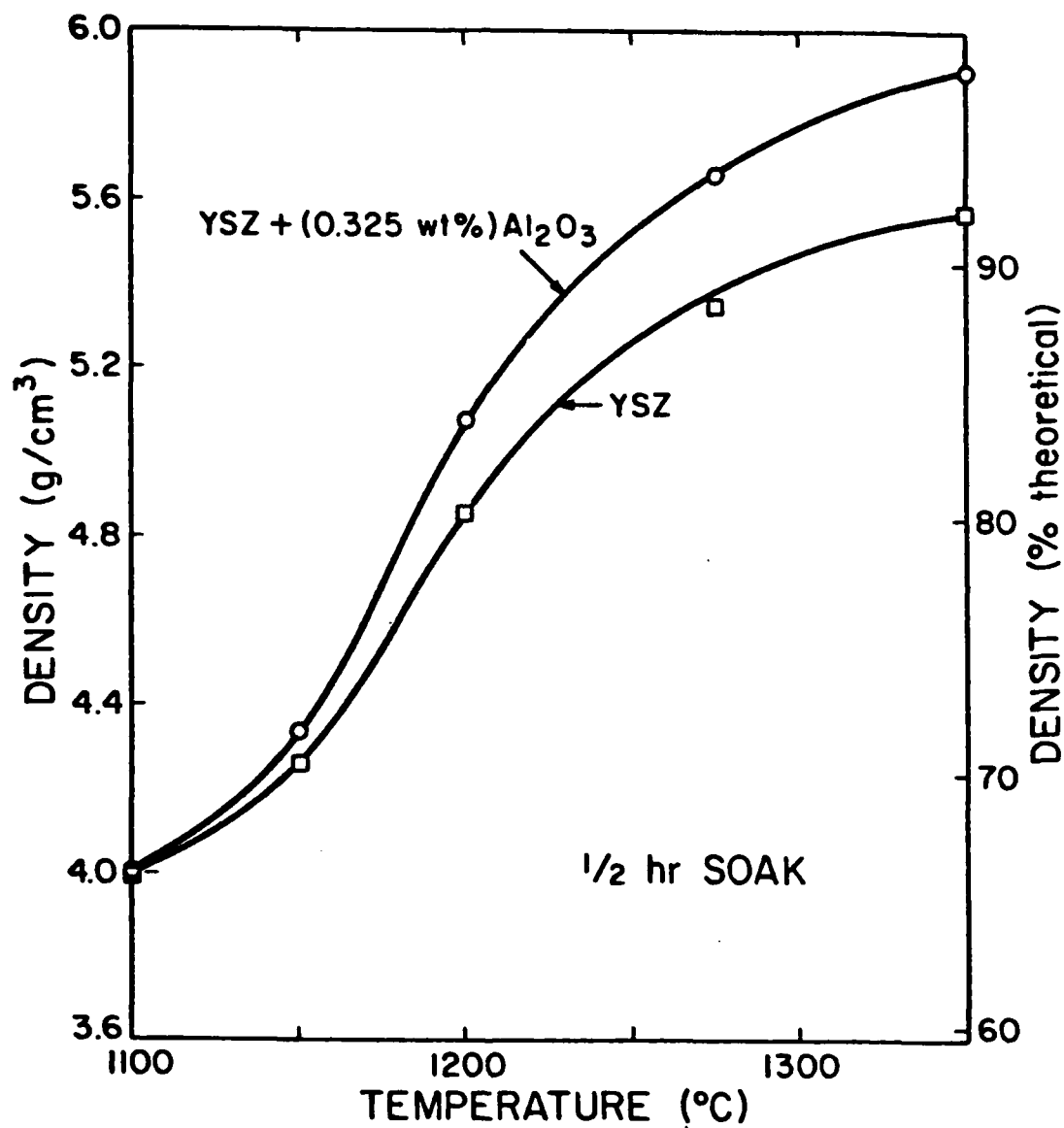


FIGURE 3. Density vs. Sintering temperature for YSZ showing sintering enhancement with temperature for Al₂O₃ additions.

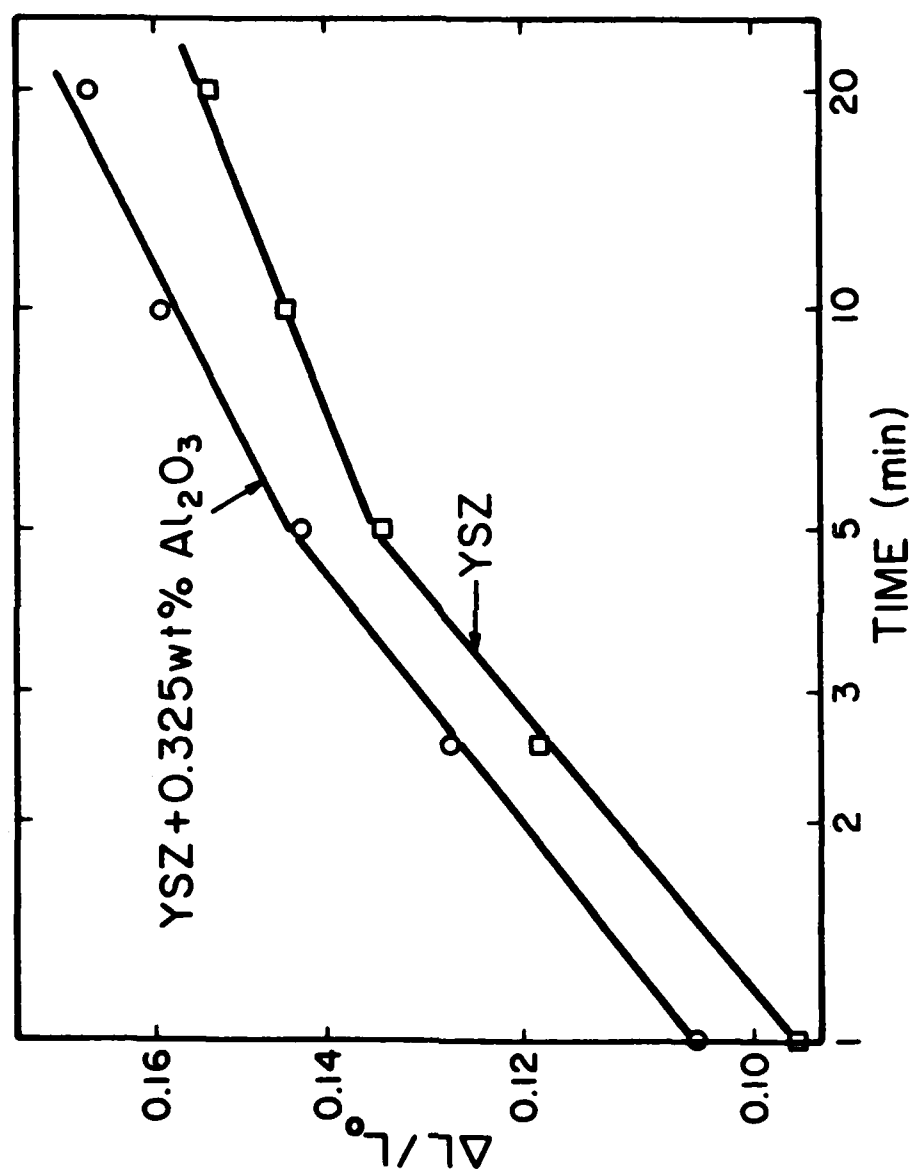


FIGURE 4. Plot of shrinkage ($\Delta L/L$) at 1275°C as a function of soak time for YSZ and YSZ + 0.325 wt% Al_2O_3 samples.

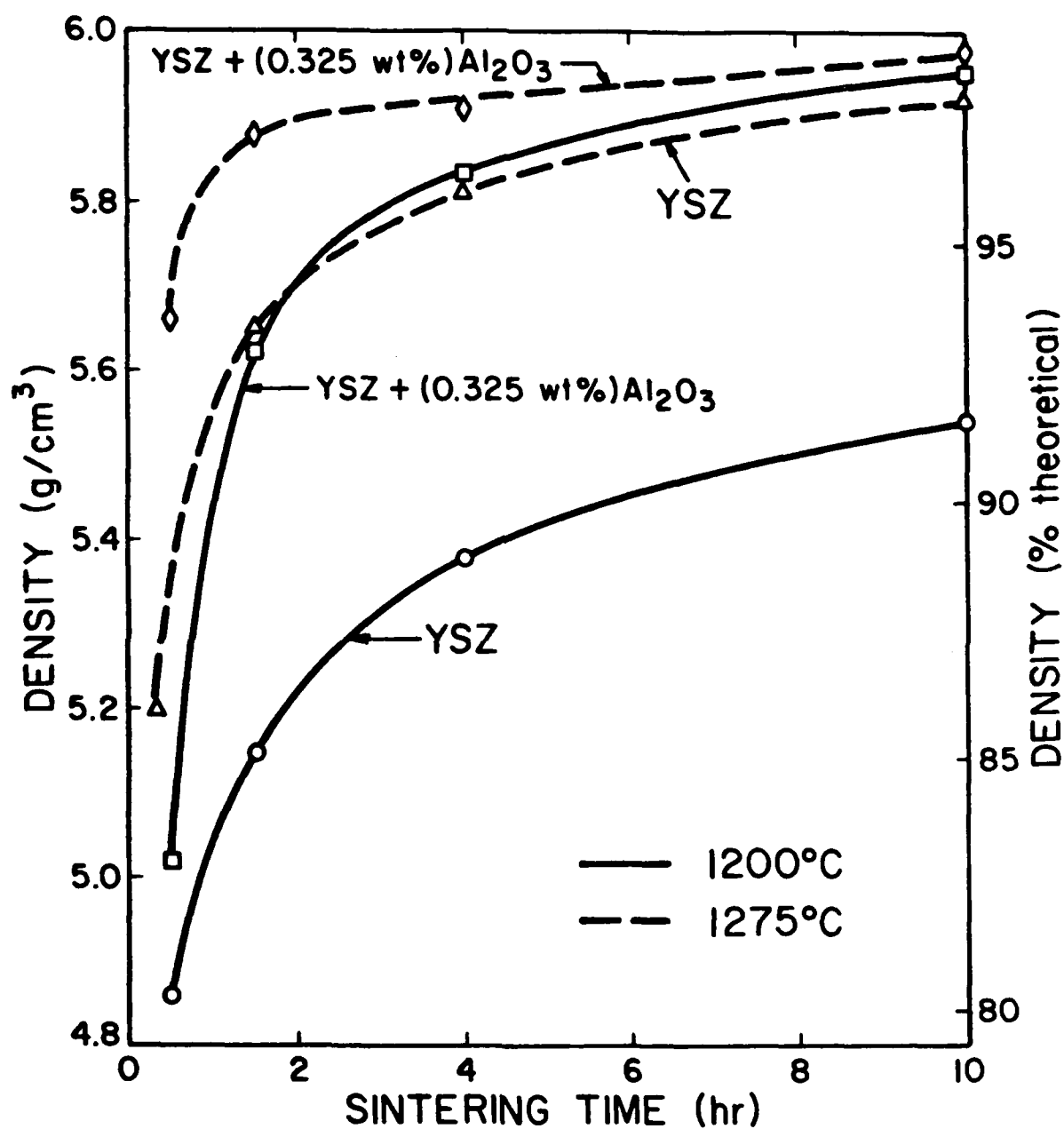


FIGURE 5. Plot of density vs sintering time for YSZ at 1200° and 1275°C showing increased densification with Al_2O_3 additions.

times (~ 0.5 hr) these density differences were much greater at 1275°C than at 1200°C , in line with the data presented in Fig. 3. In contrast, after a 10 hr. soak, the YSZ sample had achieved near equivalent density to the Al_2O_3 doped sample at 1275°C , but substantially lower density at 1200°C .

These data suggest that at 1200°C , insufficient liquid was present in either sample to cause significant rearrangement, at least in the YSZ sample, and that subsequent densification could primarily be attributed to solution precipitation and grain boundary sliding. The higher densification rate for the Al_2O_3 doped sample must, therefore, reflect the presence of a more reactive and perhaps lower viscosity intergranular phase with incorporation of Al_2O_3 . Conversely, with the higher expected liquid phase content at 1275°C , significant initial densification occurred and subsequent densification mechanisms became relatively less important, at least for the Al_2O_3 doped samples.

Fired density data are given in Table 2 for YSZ with different concentrations of Al_2O_3 additive at sintering temperatures of 1200° , 1275° and 1350°C , and for soak times of 0.5, 4.0 and 24.0 hr. The trends in the data are as illustrated in Figures 2 and 5, that is, densities generally increased with sintering temperature and soak time for all samples. The slightly lower ultimate density achieved by the samples containing 0.325 wt% Al_2O_3 (99.3% relative density compared to 99.7% for the undoped YSZ) at 1350°C was attributed to Al_2O_3 inclusions present in the sample. However, equivalent densities could generally be achieved at lower temperatures and for shorter soak times with Al_2O_3 doping.

Fig. 6 shows SEM photomicrographs of polished and thermally etched sections for the samples in Table 2 which were fired at $1275^{\circ}\text{C}/4$ hr. Fig. 6A shows the YSZ sample, with Figures 6B, 6C and 6D representing Al_2O_3 additive

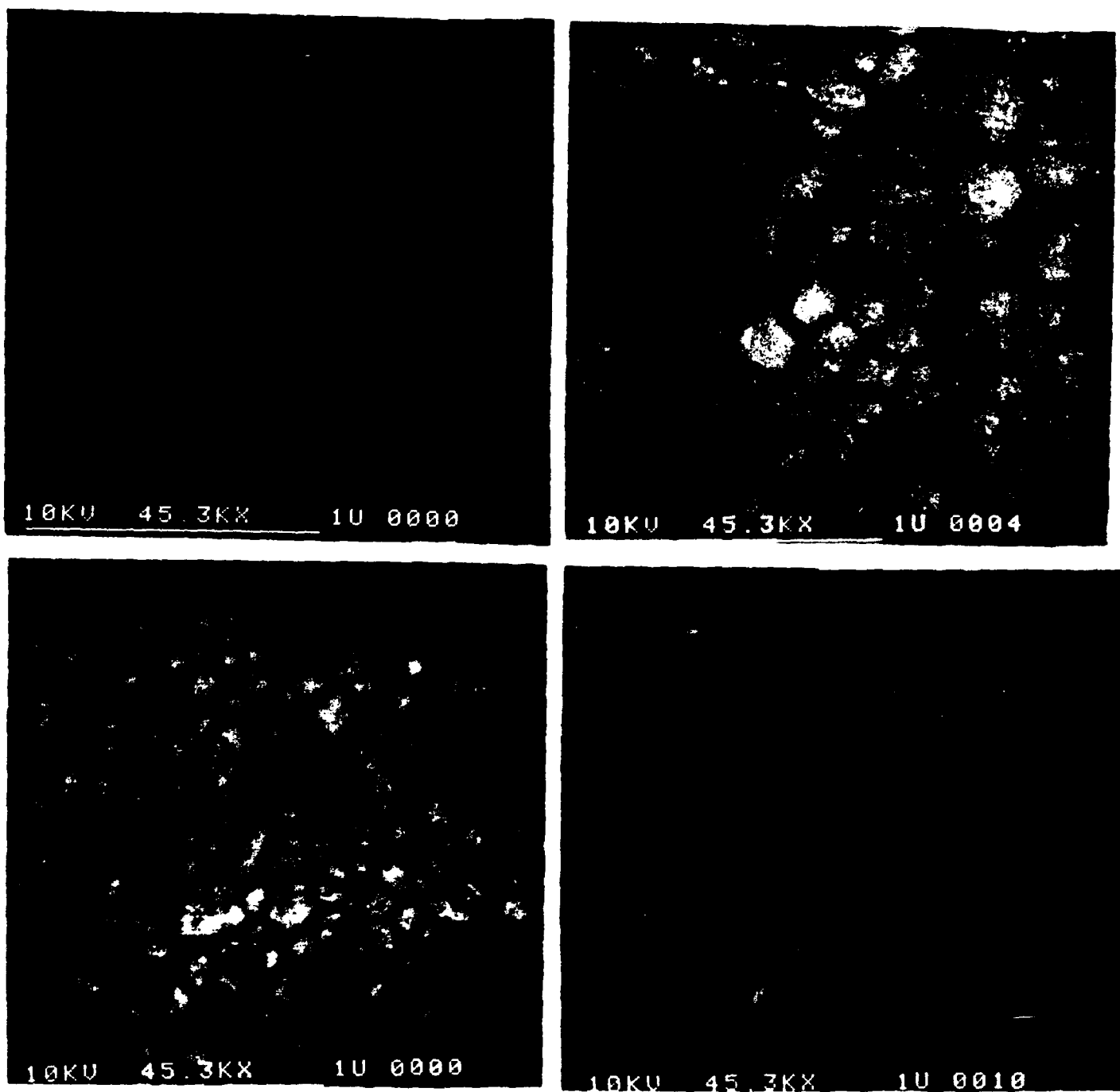


FIGURE 6. SEM photomicrographs (45.3KX) of polished and thermally etched sections of YSZ and YSZ + Al_2O_3 samples sintered at 1275°C/4 hrs. A) YSZ, B) YSZ + 0.325 wt% Al_2O_3 , C) YSZ + 0.65 wt% Al_2O_3 , and D) YSZ + 1.3 wt% Al_2O_3 .

contents of 0.325, 0.65 and 1.30 wt%, respectively. No second phases were evident from the photomicrographs presented except for few intergranular pores present in the YSZ sample. The YSZ sample also showed evidence of stacking faults in the grains, indicative of lattice strain in the sample. Stacking faults were not very evident in the YSZ samples which were doped with Al_2O_3 . This would be consistent with the existence of a liquid phase and the dissolution of Al in the ZrO_2 lattice. Indications of exaggerated grain growth were also present for the 1.3 wt% sample especially at higher sintering temperatures.

Fig. 6 shows an increase in the fired grain sizes as Al_2O_3 was added. Average grain sizes determined were approximately 0.36, 0.40, 0.38, and 0.37 μm for samples A, B, C, and D. These differences may be only marginally significant, but measurements were made on several samples. In any event, this change roughly parallels the sintering behavior (Fig. 2) and measured densities shown in Table 2, where the optimum effect on densification occurred at an Al_2O_3 additive content of 0.325 wt%. This concentration (0.325 wt%, 0.392 mol%) should nominally represent the solubility for Al_2O_3 in the YSZ structure. However, some Al_2O_3 was present as discrete particles and also dissolved in the intergranular phase. In addition, the presence of some Al_2O_3 interstitially in the YSZ structure might also be expected. The true Al_2O_3 solubility, therefore, might well be closer to that reported by Bernard (0.1 mol%).¹³

As indicated, Al_2O_3 inclusions could be found in the Al_2O_3 doped samples. These were manifested as darker areas, which EDAX analysis showed to be Al rich. Closer examination revealed these to be apparently undissolved Al_2O_3 grains or inclusions which were considerably larger than the matrix YSZ grains. These inclusions were occasionally associated with porosity, and a

perturbation of the microstructure surrounding the inclusion was also observed. The presence of Si could not definitely be identified in the perturbed region from EDAX analysis, although its presence would be expected from the work of Butler and Drennan.¹⁸ The frequency of these inclusions increased with added Al_2O_3 content above 0.325 wt%, but a few observations were made even in the undoped YSZ sample, which would indicate the presence of existing Al_2O_3 impurities.

Figure 7 shows a plot of grain size versus soak time for the YSZ and YSZ + 0.325 wt% Al_2O_3 samples. The grain size results were obtained from samples sintered 1275°C for soak times up to 24 hrs. Density data for these samples are included in Table 2. As indicated previously, the Al_2O_3 additive samples showed larger grain sizes under all conditions of equivalent densities. However, only moderate grain growth was observed between 93-99% relative density. Significant increases occurred only as near complete densification was achieved, and this was accompanied by exaggerated grain growth for the higher Al_2O_3 doped samples. This circumstance would locate the residual porosity mainly on the grain boundaries and at grain intersections, where they would be eliminated during the final grain coarsening phase. For samples showing exaggerated grain growth, lower final densities were also achieved but this would be associated with trapped intergranular porosity, since no pore phase was detected within the grains of the sintered samples.

Fig. 8 shows TEM photomicrographs of grain intersections for the YSZ and YSZ + 3.25 wt% Al_2O_3 samples at 290Kx magnification. Figures 8A and 8B represent bright field images of the respective samples. Fig. 8A (YSZ) shows clearly the existence of a liquid (X-ray amorphous) phase at the triple points and along the grain boundaries. The thin, relatively flat grain boundaries suggested a low concentration of a wetting liquid at the sintering temperature

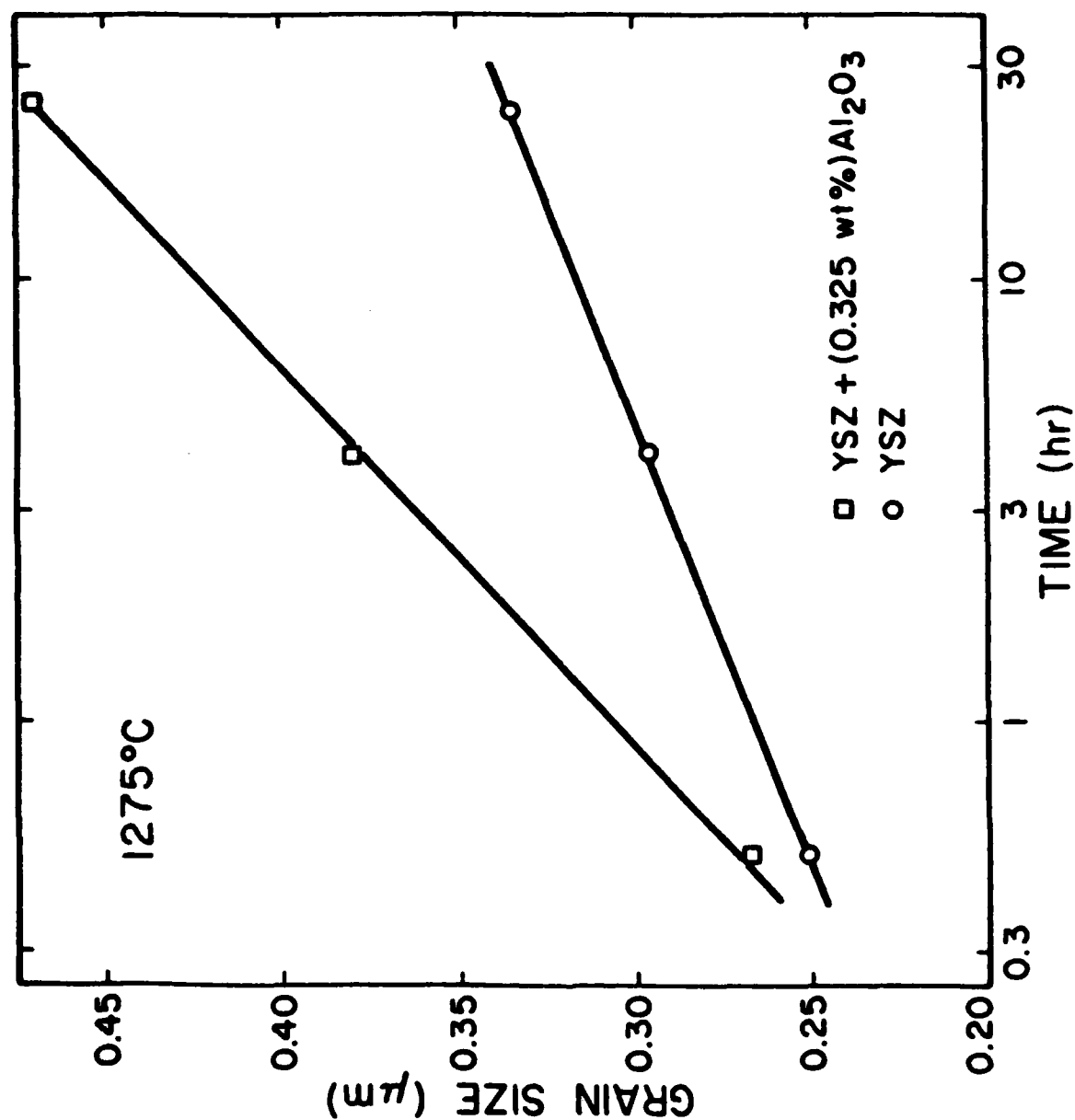


FIGURE 7. SEM photomicrographs (15 KX) of polished and thermally etched YSZ samples sintered at 1275°C/4 hrs. A) YSZ, B) YSZ + 0.325 wt% Al_2O_3 , and C) YSZ + 1.3 wt. Al_2O_3 .

Table 2

Sintered densities of YSZ and YSZ + Al_2O_3 samples for different soak temperatures and times.

Samples	Soak Time	Sintered Densities (% Theoretical)*		
	<u>(hrs)</u>	<u>1200°C</u>	<u>1275°C</u>	<u>1350°C</u>
YSZ	0.5	80.5	88.0	93.1
(6.02 g/cm ³)**	4.0	89.2	96.3	99.0
	24.0	94.0	99.2	99.7
YSZ + 0.325 wt% Al ₂ O ₃	0.5	81.1	94.1	98.3
(6.01 g/cm ³)**	4.0	97.0	98.5	99.3
	24.0	99.5	99.3	99.3
YSZ + 0.65 wt% Al ₂ O ₃	0.5	83.8	96.5	98.2
(5.99 g/cm ³)**	4.0	96.9	98.8	99.0
	24.0	99.0	99.0	99.1
YSZ + 1.30 wt% Al ₂ O ₃	0.5	80.7	96.0	97.3
(5.96 g/cm ³)*	4.0	95.8	97.8	97.6
	24.0	98.2	98.0	98.3

* Accuracy: + 0.1%

** Calculated Theoretical Densities

(1350°C). In contrast, grain boundaries for the Al_2O_3 additive samples were more rounded (Fig. 8B) and were also wider as shown in Fig. 8C (dark field image), indicative of a higher liquid phase content. Fig. 8B also showed the existence of an inclusion adjacent to the grain boundary but the boundaries otherwise appeared free of discrete second phases or inclusions.

Within the grains of the sintered samples, second phases were also not observed, although some tetragonal inclusions might have been expected considering the low yttria content of the YSZ powder (4.5 mol%). X-ray diffraction studies on the powder and fired samples likewise did not indicate the presence of a tetragonal phase, but this is normally difficult to distinguish from the cubic phase.³⁴ Only the cubic YSZ phase was identified in the samples studied and no crystalline intergranular phases were found.

EDAX spectra were obtained from the TEM samples. These were taken in the grain centers and at the triple points for the YSZ sample. These data are presented in Table 3, and show only Al and Si as significant impurities. The Si and Al average concentration in the YSZ grains were higher than the chemical analysis in Table 1 would indicate. This may reflect possible (Si) contamination during TEM sample preparation and also likely errors in the EDAX analysis. Noteworthy points from the data in Table 3 are: a) The Al and Si enrichment of the triple point regions; b) the higher overall Al concentration within grains and in intergranular regions for the Al_2O_3 doped samples; and c) the significant increase in Y concentration in the triple point regions. The concentration of Al and Si at the triple points, is consistent with the formation of a liquid boundary phase which aids in sintering. Moderate alumina enrichment of this phase would likely cause increased fluidity and enhanced sintering. Higher concentrations of yttria at the boundary phase might be expected to destabilize the YSZ structure but, as indicated, this was

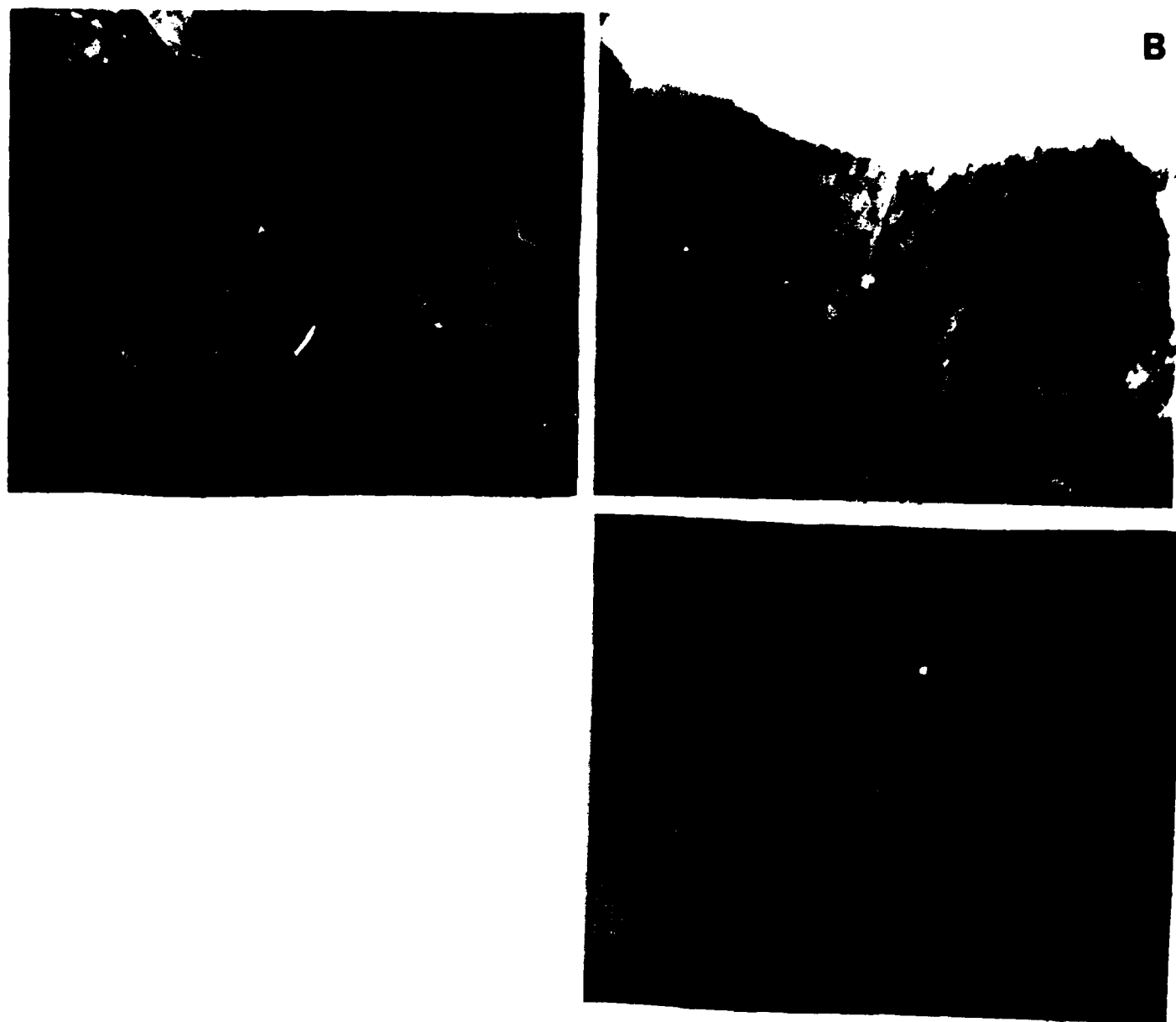


FIGURE 8. SEM photomicrograph of polished and thermally etched YSZ + 1.3 wt% Al_2O_3 sample showing. A) Al_2O_3 inclusion and D) EDAX spectra showing Al and Zr peaks.

Table 3

Elemental analysis of YSZ and YSZ + 0.325 wt% Al_2O_3 samples by EDAX technique.

Sample*	Avg. Conc. (wt %)				Location
	Al	Si	Y	Zr	
YSZ	0.28	0.99	7.42	91.09	Gr. Center
YSZ + Al_2O_3	0.56	0.97	7.69	89.51	Gr. Center
YSZ	0.36	4.56	9.77	84.86	Triple Pt.
YSZ + Al_2O_3	0.65	4.43	10.30	86.22	Triple Pt.

*Sint. Temp: YSZ - 1350°C/4h; YSZ + Al_2O_3 - 1350°C/1h.

not observed. The existence of a Y, Si, Al and Ca rich boundary phase was noted also by Moghadam et al. for a similar YSZ powder.³⁴

Fig. 9 shows a plot of electrical conductivity versus reciprocal absolute temperature for the YSZ and Al_2O_3 doped samples. The conductivity shows a significant increase with Al_2O_3 additions, though the activation energy (0.97eV) remained unchanged. A conductivity maximum at 0.325 wt% was observed, a trend similar to that noted previously for the grain size and densification behavior.

From the TEM and sintering kinetic data presented, the existence of an intergranular phase in the samples studied would seem to be well established. Densification in the submicron YSZ powders, with or without Al_2O_3 doping can, therefore, be attributed primarily to liquid phase assisted sintering, as discussed. The liquid would be formed from impurities present in the YSZ powders, which have been shown to be concentrated in the intergranular regions. It should be noted, moreover, that the impurities constitute ~0.8 wt% of the YSZ powder and were comprised primarily of such glass forming oxides as SiO_2 , Na_2O , K_2O , MgO , CaO , BaO , and Al_2O_3 . If converted into a glassy phase, this would constitute ~1.5% of the sample volume, an amount of liquid sufficient to show significant effects of liquid phase sintering.

The primary role of the added Al_2O_3 as a densification aid appears to be an enhancement in the amount and reactivity of the liquid phase at equivalent temperatures, which causes an increase in the densification rate. Within the glassy phase that might be formed from the impurity oxides present, perhaps 10-20 wt% Al_2O_3 could be dissolved, with beneficial effects on the fluidity and reactivity of the melt phase.³⁶ On this basis, less than 0.3 wt% of the Al_2O_3 would be present in the intergranular or boundary phase. Higher Al_2O_3

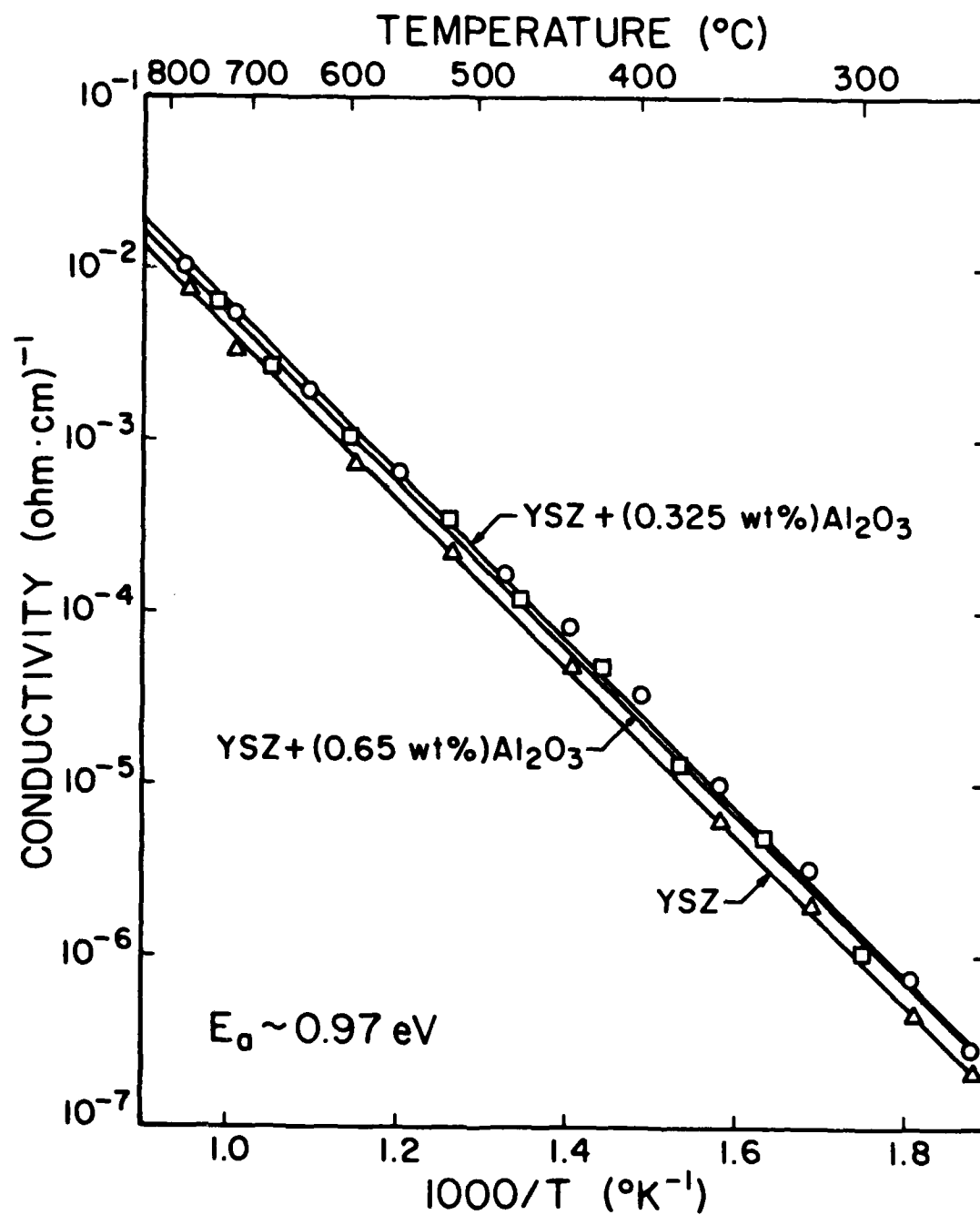


Fig. 9 DC conductivity vs. temperature for YSZ and Al₂O₃ doped samples at optimum densities.

contents would lead to a more viscous and, therefore, a less reactive melt phase. A maximum in the reactivity of the intergranular liquid as its Al_2O_3 content was varied would also explain the observed maximum in densification kinetics at the optimal (0.325 wt%) Al_2O_3 additive level. As fired grain sizes are known to be enhanced by the presence of a reactive liquid phase,³⁵ the observed similarities between grain growth behavior and densification kinetics with varying Al_2O_3 additions become evident.

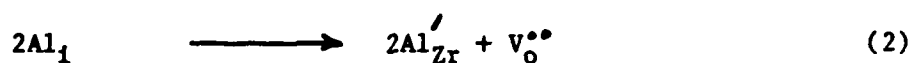
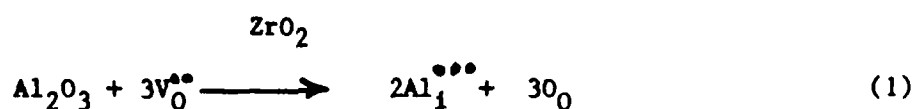
The role attributed to Al_2O_3 in the above discussion as a densification aid for submicron YSZ powders, is in general agreement with work reported by Radford and Bratton² Mallinckrodt³ and Takagi¹⁶. The authors attribute increased densification with Al_2O_3 additions to YSZ and CSZ powders to formation of an intergranular liquid phase with existing impurities, particularly SiO_2 . The Al_2O_3 was reported to be present mostly in the grain boundary phase. Radford and Bratton noted an apparent grain growth inhibition with added Al_2O_3 at 1480°C but Takagi reported a substantial increase in grain size at higher temperatures.

In contrast to the above, Bernard,¹³ Butler and Drennan¹⁸ and Rao¹⁹ all reported the presence of Al_2O_3 as discrete inclusions in zirconia. Enhanced densification was observed with the added Al_2O_3 , but the effect of the Al_2O_3 was considered by Butler and Drennan to be the scavenging of intergranular SiO_2 by Al_2O_3 inclusions with subsequent grain boundary pinning. The present study has identified Al_2O_3 inclusions in the YSZ samples but their effect on densification, at least at low concentrations, was minor.

Increased electrical conductivity was noted for YSZ samples with a low concentration (< 0.65 wt%) of added Al_2O_3 . Bernard and Verkerk et al⁷ noted this increase and attributed it to increased grain size and consequent reduction in the more resistive grain boundary area. As grain size and

conductivity behavior both reached a maximum at the 0.325 wt% additive level, this mechanism undoubtedly accounts for part of the observed increase. However, some contribution to the conduction process from the defect substitution of Al^{3+} into the YSZ lattice might also be expected.

As pointed out by Wilhelm and Howarth³⁷ in connection with the incorporation of Fe_2O_3 into YSZ, the trivalent cation can be accommodated into the lattice both interstitially and by direct substitution for Zr^{4+} as follows:



Reaction (1) represents the incorporation of alumina whereby the Al^{3+} ions would be accommodated interstitially with the suppression of existing oxygen vacancies. The cation defects would not contribute in any significant way to the conduction process, but cation mobilities would be affected. This mechanism may explain the ready dissolution of Al_2O_3 into the glassy phase. The decrease in the oxygen vacancy concentration would lower the conductivity, however, depending on the magnitude of the effect.

Reaction (2) indicates substitution of Al^{3+} ions on Zr^{4+} sites with the expected formation of oxygen vacancies. These vacancies would contribute to the conductivity, although with the initial substitution of Y^{3+} into the ZrO_2 lattice, significant oxygen vacancies would already exist.

The magnitude of these substitution effects with Al^{3+} is not known, but considering the size disparity between the Al^{3+} ($r = 0.53\text{\AA}$) and Zr^{4+} ($r = 0.84\text{\AA}$) ions, and the fact that the conductivity does increase, lattice

substitution of the Al would seem to be the dominant effect.

CONCLUSIONS

1. Sintering studies carried out on submicron YSZ powders with Al_2O_3 additives showed a significant enhancement in densification rate above 1150°C . Grain sizes, which were slightly increased by the Al_2O_3 additions, were in the range $3.5\text{--}4.0\text{ }\mu\text{m}$.
2. Densification and grain growth decreased relatively at Al_2O_3 additive levels $> 0.6\text{ wt\%}$.
3. Near-complete densification ($> 99\%$ relative density) was achieved at 1350°C in one and four hours for the $0.325\text{ wt\% Al}_2\text{O}_3$ additive and undoped YSZ, respectively. Microstructural observations and time-temperature sintering kinetics indicated that densification occurred by a liquid phase mechanism, with enhanced densification in Al_2O_3 additive samples resulting from an increased Al melt content.
4. Conductivity was increased 1.5 times by $0.325\text{ wt\% Al}_2\text{O}_3$ additions due partly to increased grain growth. Relative decreases in both grain growth and conductivity occurred at higher Al_2O_3 additive levels due to a decrease in boundary diffusion kinetics.

ACKNOWLEDGMENTS

The assistance of D. S. Phillips of the Materials Research Laboratory and Department of Metallurgy in carrying out the TEM studies is gratefully acknowledged. This work was supported by the Office of Naval Research under contract no. N-000014-80-K-0969 and in part by the National Science Foundation under MRL grant DMR-80-20250.

REFERENCES

1. H. Yanagida, M. Takata and M. Nagai, "Fabrication of Transluscent ZrO_2 Film by a Modified Doctor Blade Method," J. Am. Ceram. Soc., 65(2) C-34-C35 (1981).
2. K. C. Radford and R. J. Bratton, "Zirconia Electrolyte Cells," J. Mater. Sci., 14 (1) 59-65 (1979).
3. D. v. Mallinckrodt, P. Reynan and C. Zografou, "The Effect of Impurities on Sintering and Stabilization of ZrO_2 (CaO)," Interceram 2 (2) 126-29 (1982).
4. G. K. Layden and M. C. McQuarrie, "Effect of Minor Additions on Sintering of MgO ," J. Am. Ceram. Soc., 42 (2) 89-92 (1959).
5. W. J. Huppmann, "Sintering in the Presence of Liquid Phase," pp. 359-378 in Mater. Sci. Res., Vol. 10. Edited by G. C. Kuczynski. Plenum Press, N.Y. and London, 1975.
6. R. C. Garvie, pp. 117-66 in High Temperature Oxides, Part II. Edited by A. M. Alper. Academic Press, New York and London, 1970.
7. M. J. Verkerk, B. J. Middelhuys and A. J. Burggraaf, "Effect of Grain Boundaries on the Conductivity of High-Purity $\text{ZrO}_2\text{-Y}_2\text{O}_3$ Ceramics," Sol. State Ionics, 6 (2) 159-170, (1982).
8. N. M. Beekmans and L. Heyne, "Correlation Between Impedance Microstructure and Composition of Calcia-Stabilized Zirconia," Electrochim. Acta. 21 (4) 303-310 (1976).
9. M. Harmer, E. W. Roberts and R. J. Brook, "Rapid Sintering of Pure and Doped $\alpha\text{-Al}_2\text{O}_3$," Trans. Brit. Ceram. Soc. 78 (1) 22-25 (1979).
10. S. Prochazka and R. M. Scanlan, "Effect of Boron and Carbon on Sintering of SiC ," J. Am. Ceram. Soc., 58 (1-2) 72 (1975).

11. S. H. Chu and M. A. Seitz, "The Electrical Behavior of Polycrystalline $\text{ZrO}_2\text{-CaO}$," J. Sol. State Chem. **23**(3-4) 297-314 (1978).
12. J. E. Bauerle, "Study of Solid Electrolyte Polarization by a Complex Admittance Method," J. Phys. Chem. Solids, **30**(12) 2657-2670 (1969).
13. H. Bernard, Microstructure et Conductivite de l' Zirone Stabilisee Frittee. Ph.D. Thesis, Institut National Polytechnique de Grenoble, 1980.
14. R. C. Buchanan and A. Sircar, "Densification of Calcia-Stabilized Zirconia with Borates," J. Am. Ceram. Soc. **66** (2) C20-C21 (1983).
15. M. J. Bannister, "Development of The SiO_2 Oxygen Sensor: Sub-Solidus Phase Equilibria in the System $\text{ZrO}_2\text{-Al}_2\text{O}_3\text{-Y}_2\text{O}_3$," J. Aust. Ceram. Soc., **18**(1) 6-9 (1982).
16. H. Takagi, S. Kuwabara, H. Matsumoto, "Effects of Alumina on Sintering of Zirconia Stabilized with Calcia," Sprechsaal **107** (13) 584-88 (1974).
17. K. C. Radford and R. J. Bratton, "Zirconia Electrolyte Cells; 2, Electrical Properties," J. Mater. Sci., **14**(1) 66-69 (1979).
18. E. P. Butler and J. Drennan, "Microstructural Analysis of Sintered High-Conductivity Zirconia with Al_2O_3 Additions," J. Am. Ceram. Soc., **65** (10) 474-78 (1982).
19. B. V. Narasimha Rao and T. P. Schreiber, "Scanning Transmission Electron Microscope Analysis of Solute Partitioning in a Partially Stabilized Zirconia," J. Am. Ceram. Soc., **65**(3) C44-C45 (1982).
20. M. J. Verkerk, A. J. A. Winnubst and A. J. Burggraaf, "Effect of Impurities on Sintering and Conductivity of Yttria-Stabilized Zirconia," J. Mater. Sci., **17**(12) 3113-3122 (1982).
21. P. J. Jorgenson, "Diffusion Controlled Sintering in Oxides," pp. 401-422 in *Sintering and Related Phenomena*. Edited by G. C. Kuczynski, N. A. Hooton and C. F. Gibbon, Gordon and Breach, N.Y., 1967.

22. W. H. Rhodes and R. E. Carter, "Cationic Self Diffusion in Calcia Stabilized Zirconia," J. Am. Ceram. Soc., 49(5) 244-49 (1966).
23. M. S. Selzer and P. K. Talty, "High-Temperature Creep of Y_2O_3 -Stabilized ZrO_2 ," J. Am. Ceram. Soc., 58(3-4) 124-130 (1975).
24. M. Heughebaert-Therasse, "Contribution a L'etude de L'evolution et du Frittage de la Zircone Stabilisee par Differents Oxydes, a des Tempertures Inferieures a 1300°C," Ann. Chim., 2(4) 229-43 (1977).
25. W. S. Young and I. B. Cutler, "Initial Sintering with Constant Rates of Heating," J. Am. Ceram. Soc., 53 (12) 659-63 (1970).
26. D. Wirth, Jr., Sintering Kinetics of Ultrfine Calcia Stablized Zirconia, Ph.D. Thesis, Univ. of Illinois, 1967.
27. R. L. Coble and R. M. Cannon, "Current Paradigms in Powder Processing," pp. 151-70 in Mat. Sci. Res., Vol. II Edited by H. Palmour III, R. F. Davis and T. M. Hare. Plenum Press, N.Y. 1977.
28. A. M. Diness and R. Roy, "Experimental Confirmation of Major Change of Defect Type with Temperature and Composition in Ionic Solids," Sol. State Comm., 3(6) 123-25 (1965).
29. R. J. Brook, "Preparation and Electrical Behavior of Zirconia Ceramics," pp. 272-285 in Advances in Ceramics, Vol. 3 Edited by A. H. Heuer and L. W. Hobbs. The American Ceramic Society, Columbus, OH, 1981.
30. R. G. St. Jacques and R. Angers, "The Effect of CaO-Concentration on the Creep of CaO-Stabilized ZrO_2 ," Trans. Brit. Ceram. Soc., 72 (6) 285-289 (1973).
31. C. E. Scott and J. S. Reed, "Effect of Laundering and Milling on the Sintering Behavior of Stabilized ZrO_2 Powders," J. Am. Ceram. Soc., 58(6) 587-90 (1979).

32. W. D. Tuohig and T. Y. Tien, "Subsolidus Phase Equilibria in the System $\text{ZrO}_2\text{-Y}_2\text{O}_3\text{-Al}_2\text{O}_3$," J. Am. Ceram. Soc., 63(9-10) 595-96 (1980).
33. M. I. Mendelsohn, "Average Grain Size in Polycrystalline Ceramics," J. Am. Ceram. Soc., 52(8) 443-46 (1969).
34. F. K. Moghadam, T. Yamashita and D. A. Stevenson, "Characterization of Yttria-Stabilized Zirconia Oxygen Solid Electrolytes," pp.364-379 in *Advances in Ceramics*, Vol. 3. Edited by A. H. Heuer and L. W. Hobbs. The American Ceramic Society, Columbus, OH, 1981.
35. W. D. Kingery, "Plausible Concepts Necessary and Sufficient for Interpretation of Ceramic Grain-Boundary Phenomena: II, Solute Segregation, Grain Boundary Diffusion, and General Discussion," J. Am. Ceram. Soc., 57(2) 74-83 (1973).
36. B. Locsei, *Molten Silicates and their Properties*, Chapters 3, 4, 5 and 6. Chemical Publ. Co., N.Y. 1970.
37. R. V. Wilhelm, Jr. and D. S. Howarth, "Iron Oxide-Doped Yttria-Stabilized Zirconia Ceramic: Iron Solubility and Electrical Conductivity," Am. Ceram. Soc. Bull., 58(2) 228-32 (1979).

Summary of Work Accomplished
Under Contract No. US NAVY-N-00014-80-K-0969

1. Reports

Report issued under this contract include the following:

- a. R. C. Buchanan and S. Pope, "Optical and Electrical Properties of Yttria Stabilized Zirconia (YSZ) Crystals," (ONR Report ≤ 5), University of Illinois, Urbana, IL (September 1981).
- b. R. C. Buchanan and J. Boy, "Effect of Coprecipitation Parameters on Powder Characteristics and On Densification of PZT Ceramics," (ONR Report ≤ 6), University of Illinois, Urbana, IL (September 1982).
- c. R. C. Buchanan and D. M. Wilson, "Densification of Precipitated Yttria Stabilized Zirconia (YSZ) to Achieve Translucent Properties." (ONR Report ≤ 7), University of Illinois, Urbana, IL (November 1982).

3. Papers

- a. R. C. Buchanan and S. Pope, "Optical and Electrical Properties of Yttria Stabilized Zirconia (YSZ) Crystals," Accepted, J. of Am. Ceram. Soc., 1982.
- b. R. C. Buchanan and J. Boy, "Effect of Coprecipitation Parameters on Powder Characteristics and On Densification of PZT Ceramics," submitted to J. of Am. Ceram. Soc., 1982.
- c. A. F. Grandin de l'Eprevier and R. C. Buchanan, "Preparation and Properties of $\text{Ca}_2\text{V}_2\text{O}_7$ Single Crystals," J. Electrochem. Soc., 129, (11) 2562-65 (1982).
- d. R. C. Buchanan, H. D. DeFord, and R. W. Doser, "Effects of Vanadate Phase on Sintering and Properties of Monoclinic ZrO_2 ," Advances in Ceramics, Vol. II, [Grain Boundary Phenomena in Electronic Ceramics] American Ceramic Society (1982).
- e. A. Sircar and R. C. Buchanan, "Densification of CaO -stabilized ZrO_2 with Borate Additives," J. Am. Ceram. Soc. 66 (2) 20-21 (1983).
- f. G. Wolter and R. C. Buchanan, "Properties of Hot Pressed ZrV_2O_7 ," J. Electrochem. Soc. 130 (9) 1905-10 (1983).

- g. R. C. Buchanan & D. M. Wilson, "Role of Al_2O_3 in Sintering of Yttria Stabilized ZrO_2 Powders," Conf. on $\text{MgO}/\text{Al}_2\text{O}_3$, MIT, June, 1983 (Adv. in Ceramics).

END

FILMED

2-84

DTIC